

Supplementary Materials

Preanalytical framework for routine clinical use of liquid biopsies: combining EVs and cfDNA

Nike K. Simon^{1,2,3}, Stefanie Volz^{1,2,4}, Jussara Rios de los Rios Reséndiz^{5,6}, Tatjana Wedig^{1,2,4}, Sophia H. Montigel^{1,2,3}, Nathalie Schwarz^{1,2}, Karsten Richter⁷, Dominic Helm⁸, Michelle Neßling⁷, Lin Zielske⁵, Julia Berker^{5,6}, Sophia Russeck^{5,6}, Monika Mauermann^{1,2}, Wolf-Karsten Hofmann⁶, Stefan M. Pfister^{1,2,3,4}, Kristian W. Pajtlar^{1,2,3,4}, Kendra K. Maaß^{1,2,3,4}, Katharina Clemm von Hohenberg^{5,6}

¹Division of Pediatric Neurooncology, German Cancer Consortium (DKTK), German Cancer Research Center (DKFZ) Heidelberg, Heidelberg 69120, Germany.

²Hopp Children's Cancer Center Heidelberg (KiTZ) and NCT Heidelberg, Heidelberg 69120, Germany.

³Medical Faculty, Heidelberg University, Mannheim 68167, Germany.

⁴Department of Pediatric Oncology, Hematology and Immunology, Heidelberg University Hospital, Heidelberg 69120, Germany.

⁵Junior Clinical Cooperation Unit Translational Lymphoma Research, German Cancer Research Center (DKFZ) Heidelberg, Mannheim 68169, Germany.

⁶Department of Hematology and Oncology, Medical Faculty Mannheim, Heidelberg University, Mannheim 68167, Germany.

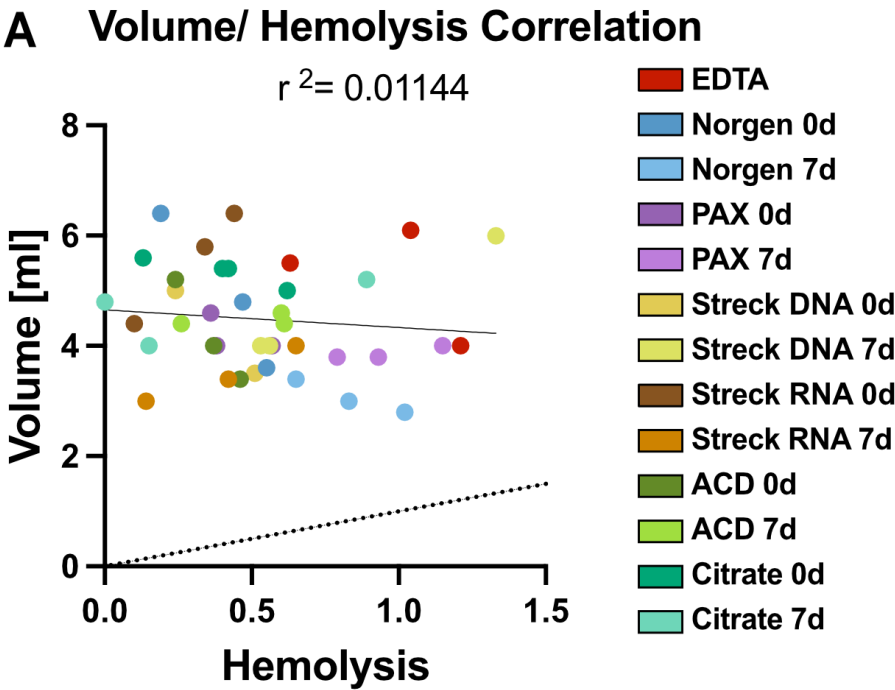
⁷Core Facility Electron Microscopy, German Cancer Research Center (DKFZ) Heidelberg, Heidelberg 69120, Germany.

⁸Proteomics Core Facility, German Cancer Research Center (DKFZ) Heidelberg, Heidelberg 69120, Germany.

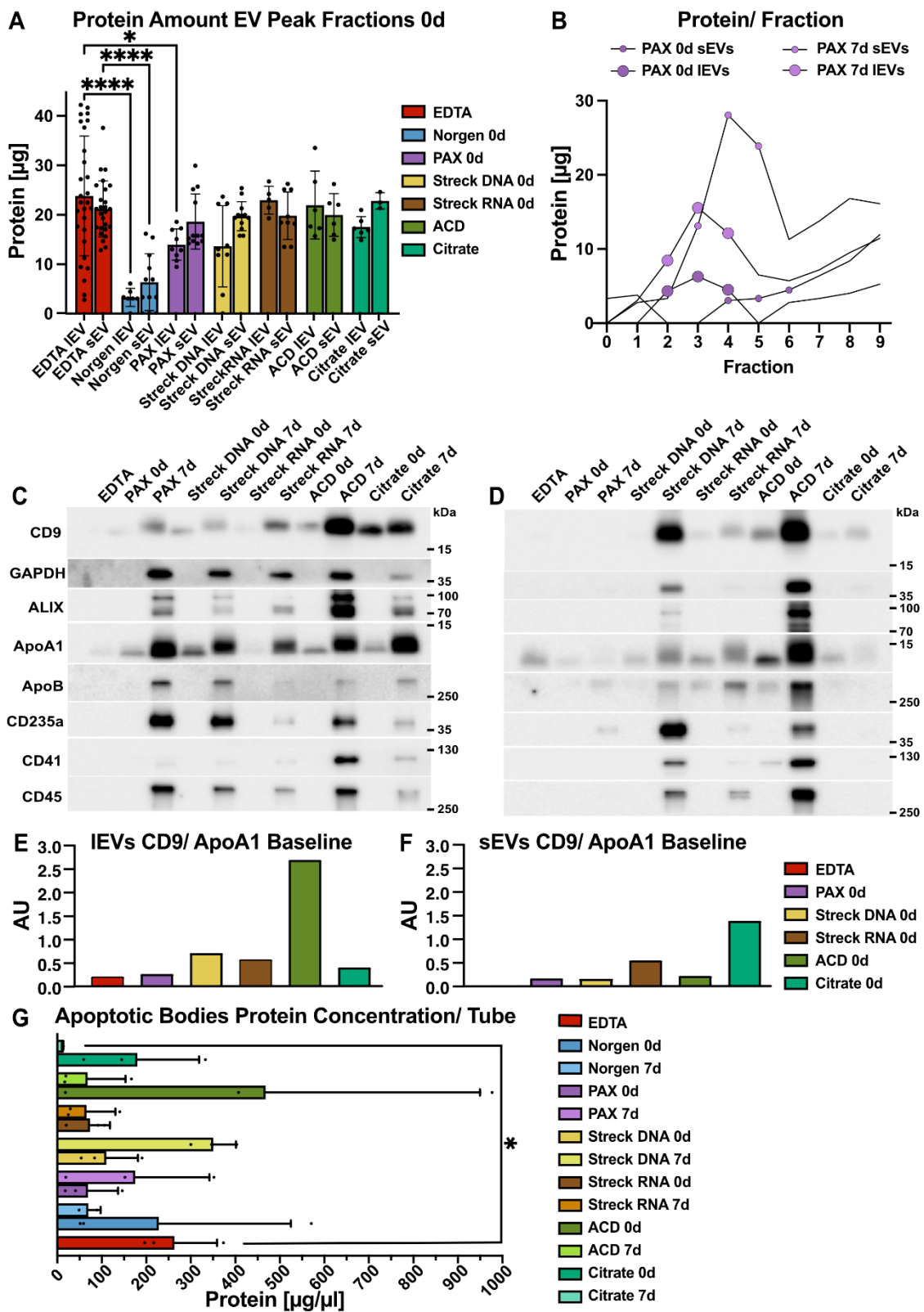
Correspondence to: Dr. Kendra K. Maaß, Junior Group Prevention and Liquid Biopsies, Hopp-Kindertumorzentrum Heidelberg (KiTZ), Heidelberg 69120, Germany. E-mail: k.maass@kitz-heidelberg.de; Dr. Katharina Clemm von Hohenberg, Junior Clinical Cooperation Unit Translational Lymphoma Research, German Cancer Research Center (DKFZ) Heidelberg, Pettenkoferstr. 22, Mannheim 68169, Germany. E-mail: k.clemm@dkfz-heidelberg.de

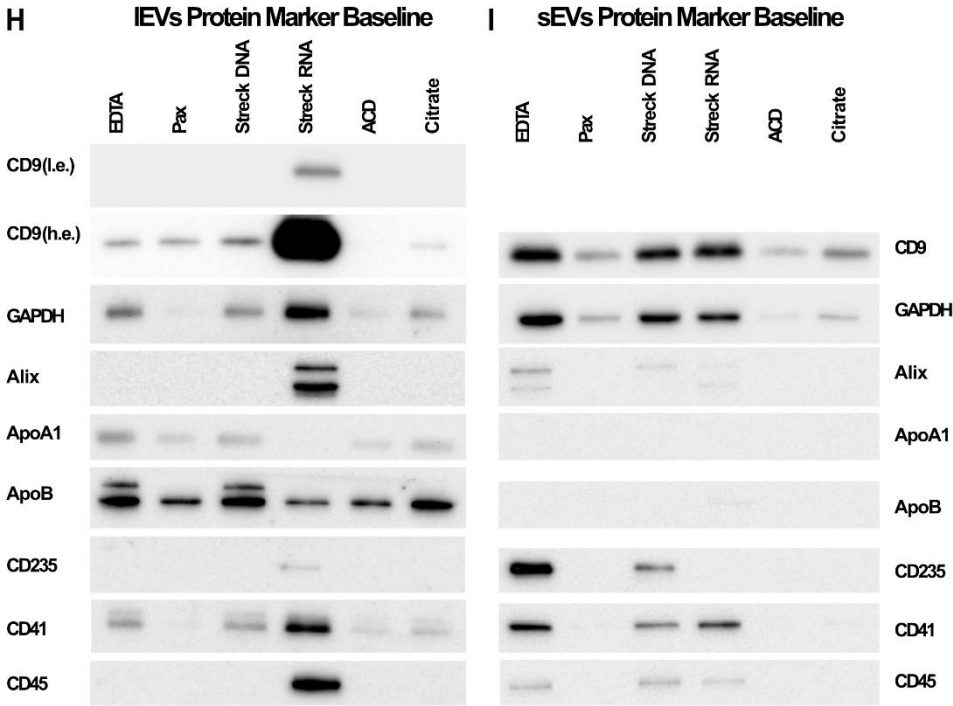
Supplementary Table 1. Characteristics of blood preservation tubes and plasma isolation parameters.

Tube	EDTA	Norgen	PAX	Streck DNA	Streck RNA	ACD	Citrate
Function	Hematological studies	DNA, RNA	DNA, RNA	DNA	RNA, EV	Blood grouping test and cell preservation	Coagulation studies
Volume	9	8,4	10	10	10	9	9
Storage Time	Max 1h	30 days at RT	14 days at RT	14 days at RT	7 days	21 days	4h
Additive	Ca Ions complexation	Osmotic cell stabilization	Biological apoptosis prevention	Chemical crosslinking	Chemical crosslinking	Acid citrate dextrose	3,2 % sodium citrate
Centrifugation	10 min	20 min	15 min	15 min	10 min	10 min	10 min
	1900 x g	500 x g	1900 x g	1600 x g	2500 x g	2500 x g	2000 x g
	4 °C	RT	RT	RT			

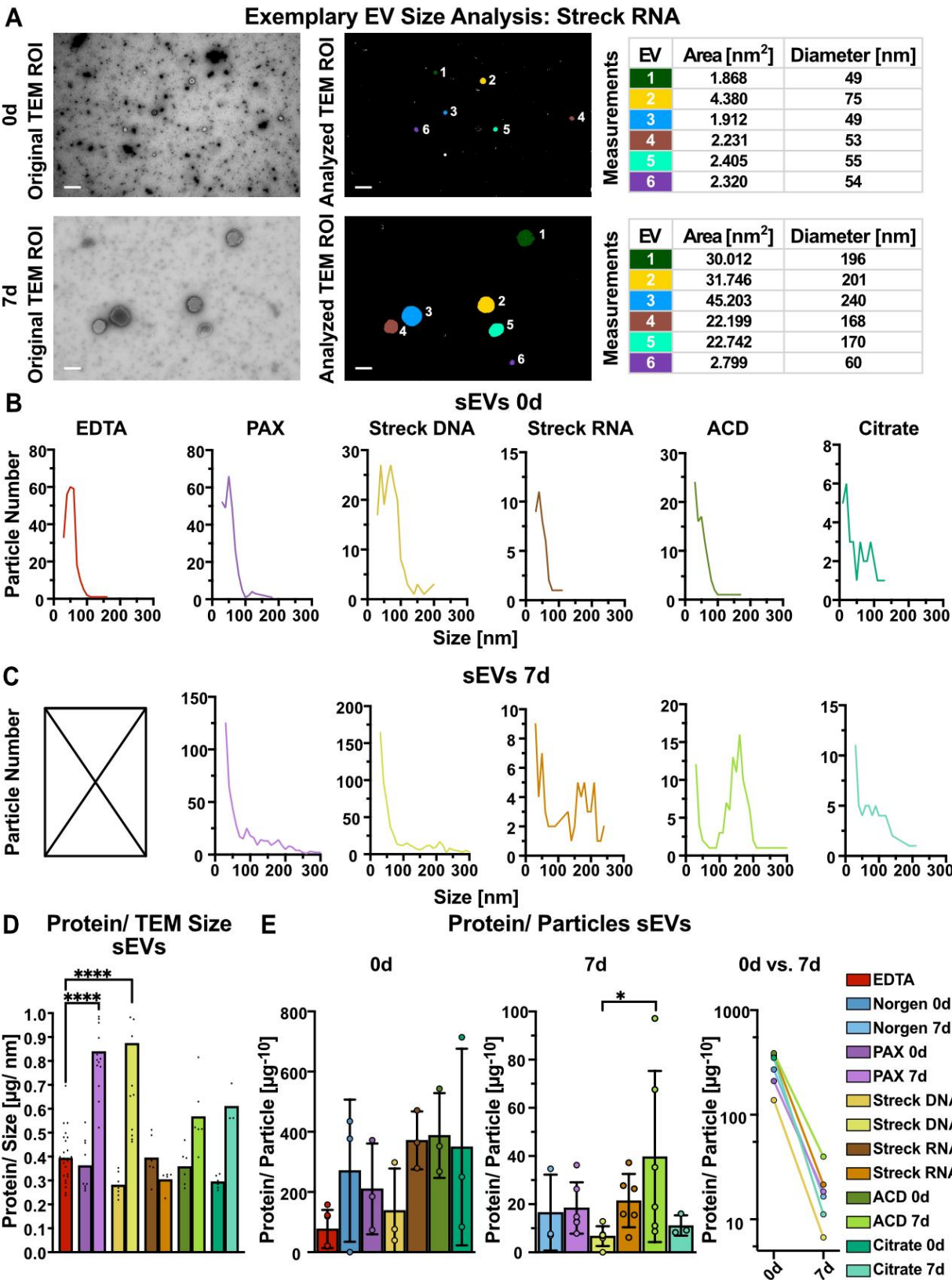


Supplementary Figure 1. Correlation of volume to hemolysis in different tube candidates (A) Correlation of plasma volume recovered from tube candidates after centrifugation and hemolysis levels determined by relative levels of free hemoglobin measured as blood plasma absorbance at 414 nm. The linear regression line is shown with 95 % confidence intervals, R^2 as depicted, $P=0.5168$.



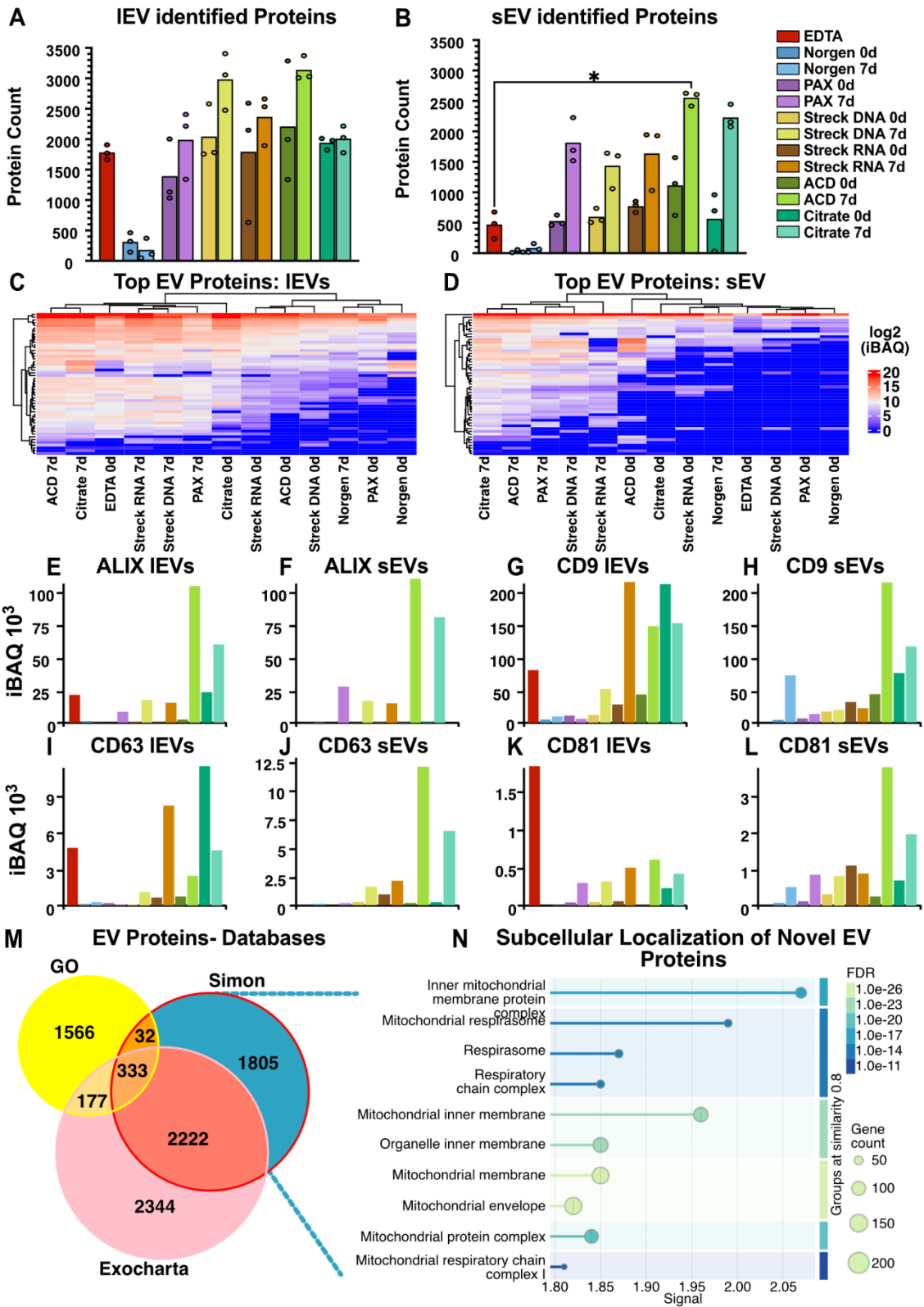


Supplementary Figure 2. Quantitative analysis of IEVs and sEVs (A) IEV and sEV protein amounts in three peak fractions per tube after immediate processing. Underlying data is identical to Figure 3A, B. (B) Exemplary protein amount profile of SEC fractions IEV and sEV collected from PAX tubes after immediate processing and after 7d highlighting the selection of the three peak fractions for IEVs 0 days (Fr. 2-4), IEVs 7 days (Fr. 2-4), sEVs 0 days (Fr. 4-6), and sEVs 7 days (Fr. 3-5). Soluble proteins are eluted in later fractions (IEVs Fr.6-9, sEVs Fr. 7-9). quantified from Western Blot data. (C, D) Western Blot analyses of pooled IEVs' and sEVs' peak fractions from three healthy individuals for classical EV marker, lipoprotein contamination and blood-derived EV marker with protein ladder sizes indicated. (G) Protein concentration of apoptotic bodies (2,000xg pellet) at baseline and after 7 days measured with BCA. (H, I) Western Blot analyses of IEVs' and sEVs' peak fractions after concentration by ultrafiltration. (E,F) Relative abundance of the EV marker CD9 and of ApoA1 as a marker for lipoprotein contamination. Statistical significance in (A) and (G) was determined using Kruskal–Wallis test, followed by Dunn's multiple comparisons test. * $P < 0.05$, **** $P < 0.0001$. Only statistically significant differences compared to EDTA are shown in the graphs; non-significant results are not marked. Norgen was excluded from the Suppl. Figure SS C, D because it fell below the threshold due to the limited sample amount. One biological replicate of Norgen 7d was excluded in Suppl. Figure S2G due to insufficient material after isolation.



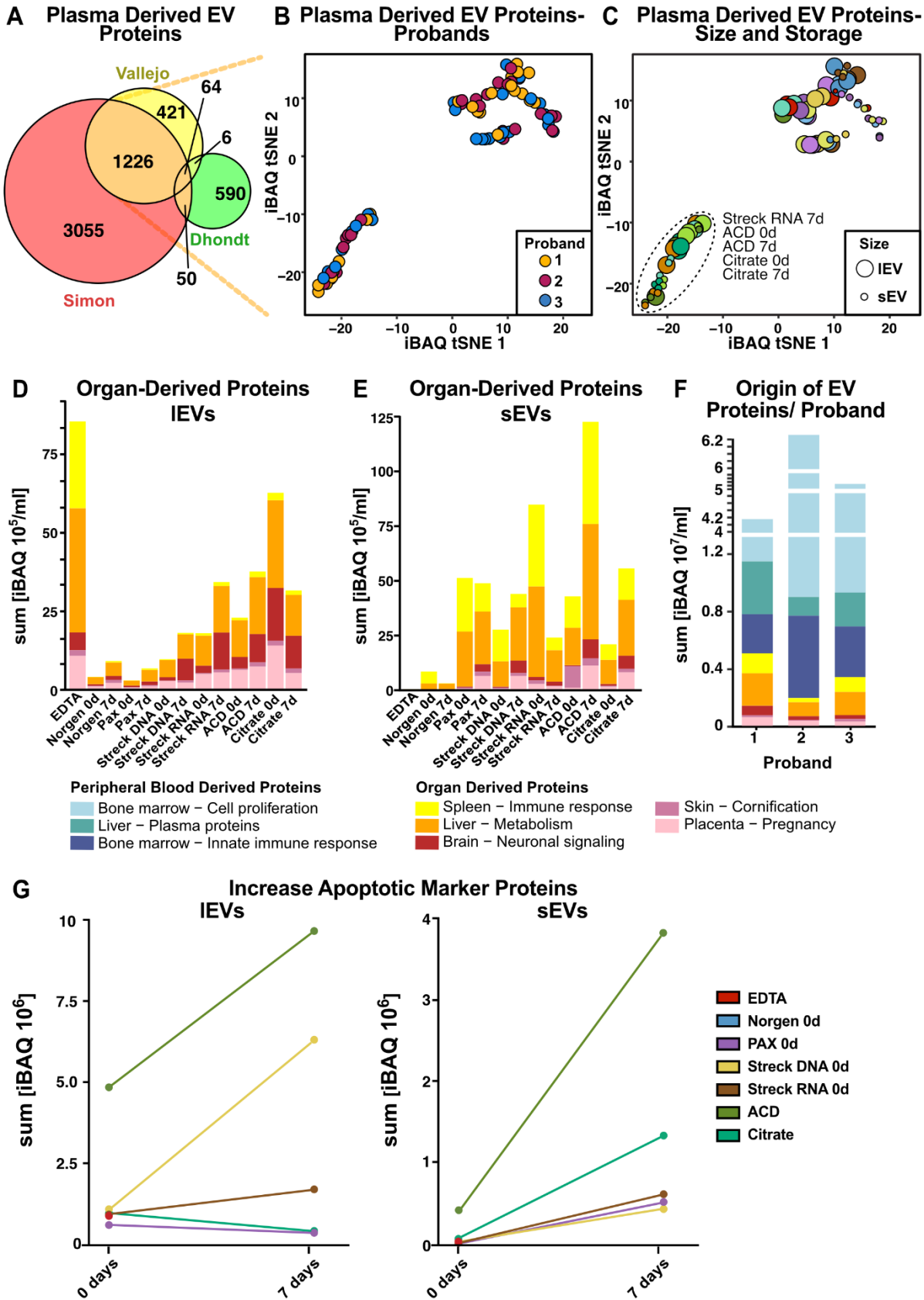
Supplementary Figure 3. Methodological comparison of size and integrity of sEVs (A) TEM image analysis of EV size of representative Streck RNA samples. Transmission electron microscopy (TEM) images were taken after immediate processing (top) and after 7d of preservation (bottom). TEM images (left) were analyzed using ilastik version 1.4.0 software to create probability maps. ImageJ was used for quantification and measurements, generating a table with depicted parameters for detected EVs (right) and

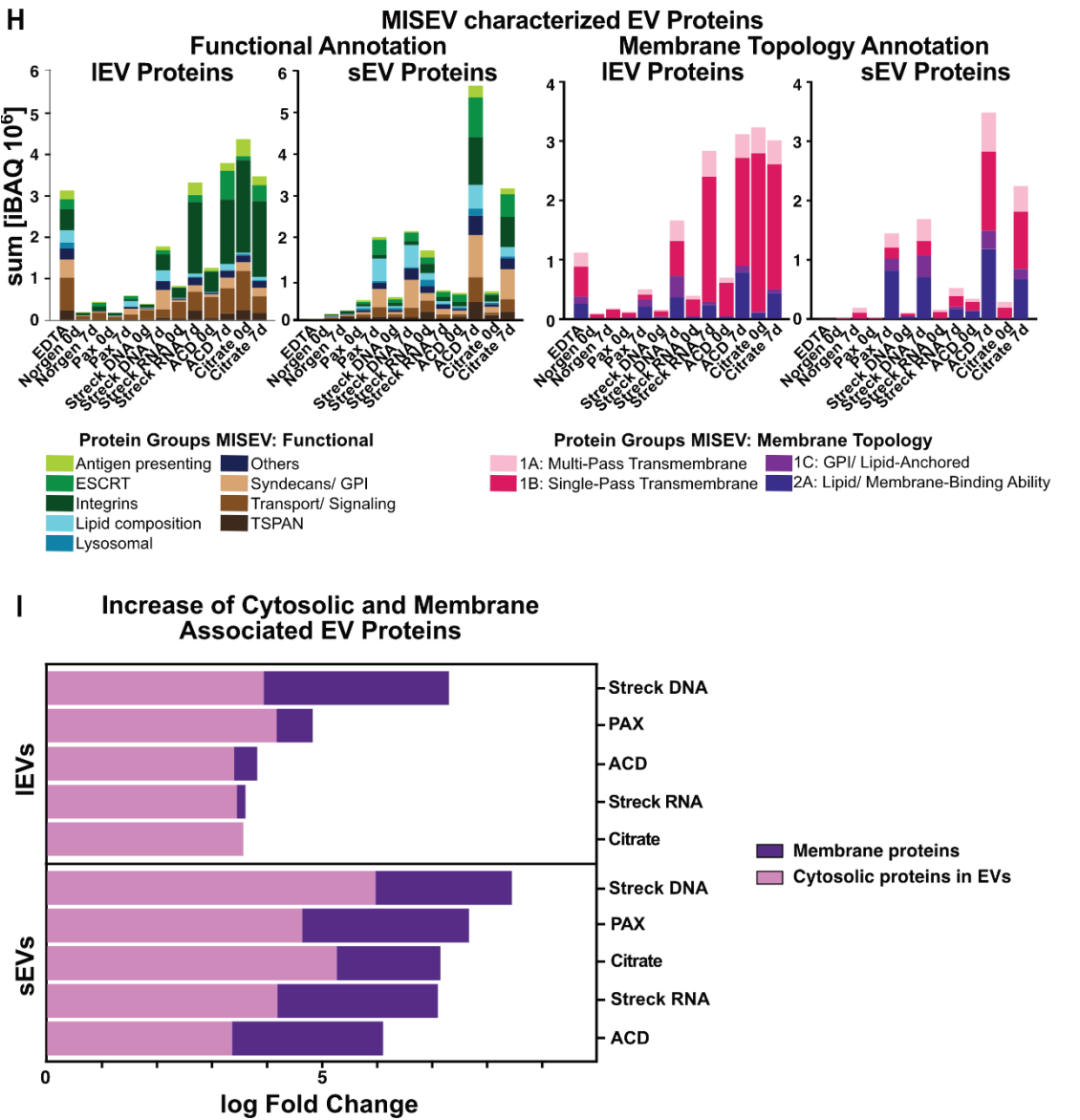
number traceable in the image (middle) (Scale bar = 200 nm). **(B-C)** Particle size distribution of sEVs after immediate processing **(B)** and after 7d **(C)** is plotted as sEV diameter measured from TEM negative stainings. **(D)** Ratio of protein per TEM sizes. **(E)** Ratio of protein per particle for each tube at baseline (left), after 7 days (middle) and time-dependent changes (right). Statistical significance for **(D)** was determined using Kruskal–Wallis test, followed by Dunn’s multiple comparisons test * $P < 0.05$, **** $P < 0.0001$. Only statistically significant differences compared to EDTA are shown in the graphs; non-significant results are not marked.



Supplementary Figure 4. Comprehensive proteome characterization of IEVs and sEVs. (A-B) Absolute numbers of identified proteins in IEV (A) and sEV (B) peak fractions. (C) IEVs and (D) sEVs heatmaps displaying the summed iBAQ values for indicated tube types and preservation times of 51 proteins abundant in our samples that overlap with the top 100 EV proteins according to the Vesiclepedia database(1). (E-L) Summed iBAQ values of all IEV and sEV samples of indicated tube types at baseline and after 7d for ALIX (E, F), CD9 (G, H), CD63 (I, J), CD81 (K, L). (M) Venn diagram illustrating the number of identified proteins by mass spectrometry and their overlap with GO Term and Exocharta(2) EV

protein lists. (N) STRING(1, 3) analysis of the subcellular localization of proteins not overlapping with neither GO term nor Exocharta EV protein list. Statistical significance for (A) and (B) was determined using Kruskal–Wallis test, followed by Dunn’s multiple comparisons test * $P < 0.05$





Supplementary Figure 5. Deciphering EV protein origin by mass spectrometry (A) Venn diagram illustrating the number of proteins by mass spectrometry and their size-adjusted overlap with Vallejo *et al.*(4) and Dhondt *et al.*(5). (B, C) t-SNE clustering of three different probands (B) and different tube types, sizes and storage times (C) depicting plasma derived IEV and sEV proteins defined by the overlap of proteins in all EV protein lists (Vallejo, Dhondt and Simon, indicated in (A)). (D, E) Organ-derived origin estimation of proteins identified in (B) IEVs and (C) sEVs. (F) Tissue origin estimation of identified proteins in three different probands in all tubes. (G) Increase of apoptotic marker proteins iBAQ values over time. (H) Functional annotation of proteins according to MISEV(6) protein characterization for IEVs and sEVs (left) and membrane topology annotation according to MISEV(6) protein characterization for IEVs and sEVs (right). (I) iBAQ log fold change of transmembrane (or GPI-anchored) proteins associated with plasma membrane and/or endosomes proteins (dark purple) and cytosolic EV proteins (light purple) over storage for 7d vs. 0d. Norgen was excluded from the Fig. S5H, because it fell below the threshold due to the limited protein amount isolated.

REFERENCES

1. Chitti SV, Gummadi S, Kang T, Shahi S, Marzan AL, Nedeva C, et al. Vesiclepedia 2024: an

extracellular vesicles and extracellular particles repository. *Nucleic Acids Res.* 2024;52(D1):D1694-d8. doi: 10.1093/nar/gkad1007. PubMed PMID: 37953359; PubMed Central PMCID: PMC10767981.

2. Mathivanan S, Fahner CJ, Reid GE, Simpson RJ. ExoCarta 2012: database of exosomal proteins, RNA and lipids. *Nucleic Acids Res.* 2012;40(Database issue):D1241-4. Epub 20111011. doi: 10.1093/nar/gkr828. PubMed PMID: 21989406; PubMed Central PMCID: PMC3245025.

3. Szklarczyk D, Kirsch R, Koutrouli M, Nastou K, Mehryar F, Hachilif R, et al. The STRING database in 2023: protein-protein association networks and functional enrichment analyses for any sequenced genome of interest. *Nucleic Acids Res.* 2023;51(D1):D638-D46. doi: 10.1093/nar/gkac1000. PubMed PMID: 36370105; PubMed Central PMCID: PMC9825434.

4. Vallejo MC, Sarkar S, Elliott EC, Henry HR, Powell SM, Diaz Ludovico I, et al. A proteomic meta-analysis refinement of plasma extracellular vesicles. *Sci Data.* 2023;10(1):837. Epub 20231128. doi: 10.1038/s41597-023-02748-1. PubMed PMID: 38017024; PubMed Central PMCID: PMC10684639.

5. Dhondt B, Pinheiro C, Geeurickx E, Tulkens J, Vergauwen G, Van Der Pol E, et al. Benchmarking blood collection tubes and processing intervals for extracellular vesicle performance metrics. *J Extracell Vesicles.* 2023;12(5):e12315. doi: 10.1002/jev2.12315. PubMed PMID: 37202906; PubMed Central PMCID: PMC10196222.

6. Welsh JA, Goberdhan DCI, O'Driscoll L, Buzas EI, Blenkiron C, Bussolati B, et al. Minimal information for studies of extracellular vesicles (MISEV2023): From basic to advanced approaches. *J Extracell Vesicles.* 2024;13(2):e12404. doi: 10.1002/jev2.12404. PubMed PMID: 38326288; PubMed Central PMCID: PMC10850029.